PHYSICAL REVIEW E VOLUME 56, NUMBER 6 DECEMBER 1997

Soft-mode turbulence in electrohydrodynamic convection of a homeotropically aligned nematic layer

Yoshiki Hidaka, Jong-Hoon Huh, Ken-ichi Hayashi, and Shoichi Kai
Department of Applied Science, Faculty of Engineering, Kyushu University, Fukuoka 812-81, Japan

Michael I. Tribelsky
Graduate School of Mathematical Sciences, University of Tokyo, 3-8-1 Komaba, Meguro-ku, Tokyo 153, Japan

(Received 13 August 1996; revised manuscript received 17 January 1997)

The experimental study of electroconvection in a homeotropically aligned nematic (MBBA) is reported. The system undergoes a supercritical bifurcation ''rest state-spatiotemporal chaos.'' The chaos is caused by long-wavelength modulation of the orientation of convective rolls. For the first time the observations both below and beyond the Lifshitz point are accompanied by quantitative analysis of temporal autocorrelation functions of turbulent modes. The dependence of the correlation time on the control parameter is obtained. A secondary bifurcation from normal to abnormal rolls is discussed. [S1063-651X(97)51412-7]

PACS number(s): 47.27.Cn, 47.52.+j, 47.65.+a, 61.30.Gd

Being a rich pattern-forming system, ac-driven electrohydrodynamic convection (EHC) in a nematic layer attracts a good deal of attention of both theoreticians and experimentalists [1,2]. The system consists of a thin layer of a nematic liquid crystal sandwiched between two parallel electrodes. The convection occurs when the applied to the layer ac voltage V exceeds a certain threshold V_c [3]. There are two conventional realizations of EHC, namely planar, where the director $\mathbf{n}$ lies in plane of the electrodes (x-y plane), and homeotropic, where the director is perpendicular to the electrodes. It is clear that in the planar alignment the nonconvective state is anisotropic in the x-y plane, contrary to the homeotropic geometry, where spatially uniform distribution of the director parallel to the z axis yields isotropy in the x-y plane.

In EHC most attention has been paid to the planar orientation; the homeotropic alignment has not been studied in detail yet. Meanwhile, in the homeotropic case EHC instability is usually preceded by Fréedericksz transition: beyond a certain threshold voltage V_F the director tilts with respect to the z axis [3]. Thus, at $V>V_F$ the director has a nonzero projection on the x-y plane ($\mathbf{n}_\parallel$), which therefore brings about spontaneous breaking of isotropy in this plane. Since orientation of $\mathbf{n}_\parallel$ is not imposed by any external factor, the system is degenerate with respect to arbitrary rotations in the x-y plane. In other words, at the threshold of homeotropic EHC the system has additional (compared to the planar alignment) continuous one-parameter group of symmetry, which provides grounds for qualitatively different dynamics.

Theoretical analysis of pattern formation at small values of the normalized control parameter [$\varepsilon \equiv (V^2-V_c^2)/V_c^2 \ll 1$] shows that planar and homeotropic EHC do differ dramatically [4,5]. In particular, in the planar case at small ε one can have steady stable normal rolls (the pattern's wave vector $\mathbf{k}$ is parallel to undistorted $\mathbf{n}$) at the frequency of the applied ac-voltage f lying beyond the so-called Lifshitz point (LP), and oblique rolls (a certain finite angle between $\mathbf{k}$ and $\mathbf{n}$) below LP [1,2].

Contrary to this, in the homeotropic case while beyond LP the governing equations also have steady solutions of the normal-roll type; all of them are unstable under very general conditions [5]. The instability occurs due to coupling of the roll-pattern with a band of slowly evolving long-wavelength modes originated in the degeneracy of the system. The situation is similar to that discussed earlier for the ''free-slip'' convection [6], or in more general terms in Refs. [7,8]. Below LP any steady oblique-roll solution merely does not exist, since the torque on $\mathbf{n}_\parallel$ exited for the oblique rolls cannot be compensated [5]. These peculiarities of the problem make it reasonable to expect the system to undergo direct transition from the nonconvective state to spatiotemporal chaos (STC) [5,9–12].

Note, STC at onset (or close to onset) of the very first hydrodynamic motion was known before, e.g., in systems undergoing Hopf bifurcation supplemented with the Benjamin-Feir destabilization [2], or in Rayleigh-Bénard convection in a rotating container [2,13] (see also Refs. [14–16] for more recent results). In all these cases STC is associated with destabilization of a pattern by *short-wavelength* modes whose wave numbers are close to that for the pattern itself. In contrast STC at onset of homeotropic EHC is caused by *continuous long-wavelength* modulation of the orientation of convective rolls (see below), which makes it qualitatively different from the above-mentioned examples.

Computer simulations of dynamics of the homeotropic EHC at onset indicate exponential decay of temporal autocorrelation functions with the correlation time τ scaled as ε^{-1} both below and beyond LP [5]. The same dependence $\tau(\varepsilon)$ is obtained in the sophisticated study of direct transition to STC governed by a generalized one-dimensional Burgers equation with short-wavelength instability and slow long-wavelength dynamics presented in Refs. [7], and probably is the generic feature of STC arising from a trivial (spatially uniform) state as a result of a single supercritical bifurcation.

It should be emphasized that while in the Ginzburg-Landau equation, which describes pattern formation, e.g., in planar EHC, dependence $\tau \propto \varepsilon^{-1}$ follows from trivial rescaling of the variables, which reduces the problem to an ε-free form, it is not the case in both the above-mentioned examples [5,7,8]. In these problems ε cannot be scale out entirely and always enters the governing equations explicitly [17]. It makes the law $\tau \propto \varepsilon^{-1}$ much less obvious.

Supercriticality of the bifurcation accompanied with divergence of the correlation time at $\varepsilon=0$ allows one to merge the STC with the trivial state both by vanishing amplitudes of the turbulent modes and by slowing down their temporal evolution. Since the mentioned properties of transition to STC in the homeotropic EHC resemble those well-known for the so-called soft modes in kinetics of second-order phase transitions, it motivates us to name the phenomenon *soft-mode turbulence* (SMT).

We use the nematic liquid crystal p-methoxybenzilidene-p'-n-butylaniline (MBBA), which is filled between two parallel glass plates whose surfaces are coated with transparent electrodes, indium tin oxide (ITO). The space between the glass plates is maintained with polymer spacers of 50 μm and the lateral size of the space is of 1×1 cm^2. Thus, the aspect ratio of the convective system in the present study is 200. In order to realize homeotropic alignment surfaces of the glass plates are treated by a surfactant (n-n'-dimethyl-n-octadecyl-3-aminopropyl-trimethoxy silyl chloride: DMOAP). When a constant magnetic field is applied parallel to the glass plate, the threshold for magnetically induced Fréedericksz transition is $H_F=1100$ G. The threshold value for electrically induced Fréedericksz transition is $V_F=3.92$ V independently of the applied frequency (up to 5 kHz). The conductivities of the MBBA are $\sigma_\parallel=3.30\times10^{-7}$ Ω^{-1}/m and $\sigma_\perp=2.34\times10^{-7}$ Ω^{-1}/m, respectively [controlled by 0.012 wt%-doping of tetra-n-butyle-ammonium bromide (TBAB)]. The critical frequency f_c of the applied electric field is about 2.6 kHz. The dielectric constants are $\epsilon_\parallel=4.21$ and $\epsilon_\perp=4.70$, i.e., $\epsilon_a=-0.49$. The temperature is controlled at 30 ± 0.02 °C with a control stage and a double-wall copper cavity. An ac-voltage is applied to the sample employing an electronic synthesizer controlled by a computer. SMT is observed at different frequencies of the applied voltage ($f=100$, 500, 1000, 1500, and 2000 Hz). All images are taken by a charge coupled device (CCD) camera and stored onto a magnetic tape as well as a magnetic disk for later analysis by a computer. The software used for image analysis is the NIH-image.

The experimental procedure is as follows. First, V is raised at once from zero to a certain V_1 from the range $V_F<V_1<V_c$ to generate Fréedericksz transition in the nonconvective state. This voltage is fixed for 50–60 min until the nematic reaches the equilibrium Fréedericksz distortion. Then the voltage is raised again to a desired value $V=V_2>V_c$ to trigger convective dynamics. The images are taken during the first 5 min after the voltage jump from V_1 to V_2 in order to study transition from the nonconvective state to SMT and then, after a 50–60 minute pause, to study the asymptotic state of the system. After removal of the applied voltage we also wait for 50–60 min to erase ''memories'' of the previous experiment before the beginning of a next set of observations, i.e., each time the system is perfectly reseted.

In works [10] the chaotic states close to onset below and beyond LP may be locally regarded as distorted oblique and normal rolls, respectively. In our experiments, it is true only for transient patterns observed just after the voltage jump from $V_1<V_c$ to $V_2>V_c$, see the first snapshots in Fig. 1. These patterns are associated with growth of unstable short-

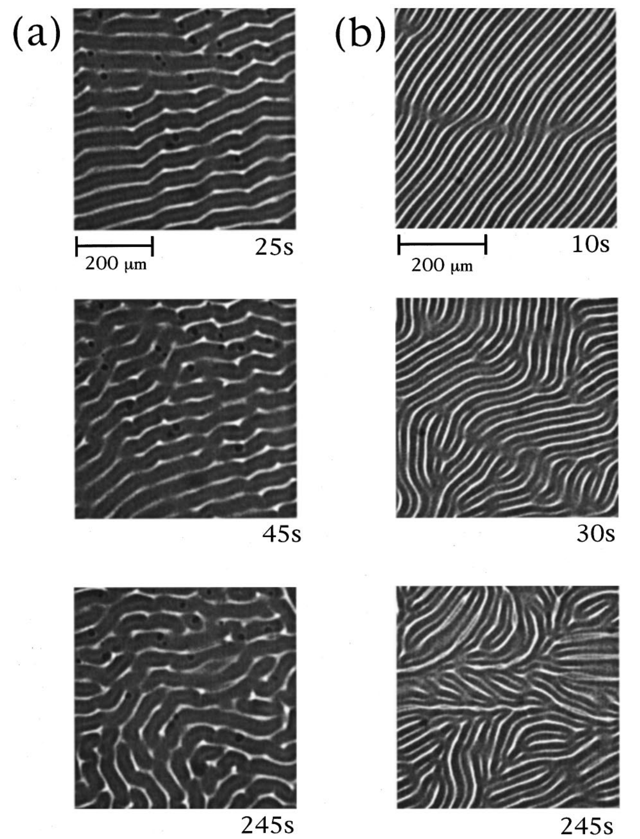

FIG. 1. Transition to soft-mode turbulence in homeotropic EHC below the Lifshitz point [(a) $f=100$ Hz, $\varepsilon=0.10$] and beyond it [(b) $f=2000$ Hz, $\varepsilon=0.10$]; snapshots of patterns in successive moments of time (indicated below the images) after the voltage jump from $V_1<V_c$ to $V_2>V_c$.

wavelength perturbations undergoing in the initial, practically, spatially uniform azimuthal distribution of $\mathbf{n}_\parallel$. However, later the transient patterns are always destroyed by growth of slowly evolving long-wavelength perturbations. It gives rise to the transition of the system to asymptotical states, which in all the examined cases are quite different from both oblique- and normal-roll patterns; see Fig. 1.

Two important qualitative results obtained in the experiments are as follows. First, while transient patterns may in addition to short-range ordering exhibit also long-range one (normal- or oblique-roll type, depending on the frequency) imposed by the initial conditions, the asymptotic states of the system are always long-range disordered; only short-range roll-like ordering remains (see Fig. 1). Second, the asymptotic states are always (i.e., below LP as well as beyond it) *dynamical*: the corresponding patterns slowly evolve in time without any tendency to reach a steady state. We emphasize both the results (viz., the long-range disorder of the asymptotics states and their unsteadiness) are valid at all the above-mentioned values of f and at any, even the smallest examined values of ε (less than 10^{-2}) [18]. The long-range disorder of the asymptotic states is associated with variation of the azimuthal orientation of the local wave vector of rolls. The variations occurs through the whole 2π angle without any preferable direction in the x-y plane; see the last snapshots in Fig. 1. It results in *spatial isotropy* of the observed STC (see also the spatial spectrum of the SMT presented in Fig. 3, Ref.[12]).

A constant magnetic field H applied in the layer's plane lifts the degeneracy of the system in this plane and hence has to stabilize both normal and oblique rolls [4,5], so that the corresponding long-range ordering has to be restored. The stabilization is indeed observed in our experiments in agreement with earlier publications [10–12]. The effect is reversible with respect to the magnetic field, as soon as it is removed the system returns to the STC, which also agrees with the results of Refs. [10,11].

An important statistical characteristic of any random process is its autocorrelation function $\phi(t)$. In our experiments the autocorrelation functions are obtained for the asymptotic states of the system at $H=0$ and two different values of the frequency, namely $f=500$ Hz (below LP) with the corresponding V_c equals 8.34 V and $f=2000$ Hz (above LP), $V_c=12.43$ V [19]. The value of V_1 is fixed at 6.00 V. Regarding V_2, it was different in different experiments in order to obtain ε dependence of the autocorrelation functions. The following technique is employed. First, in the recorded two-dimensional snapshots the same arbitrary line, defined as x axis, whose particular orientation is no matter due to the mentioned isotropy of the STC, is selected. Then, the images of this line are digitized to one-dimensional profiles of the intensity of 512 pixels with the brightness of 256 gray values, and the 256 one-dimensional profiles are sampled at 1.0 s and placed from the top to the bottom in a chronological order [20]. Next, for all the spatial points x from the spatiotemporal images the local temporal autocorrelation functions $\phi_x(t)$ are computed by averaging of the corresponding expression over the total observation time T. Finally, to smoothen random errors caused by finiteness of T, the obtained set of functions $\phi_x(t)$ is averaged over x, and the result is regarded as the true autocorrelation functions $\phi(t)$. All the obtained autocorrelation functions fall off rapidly to zero, which is typical of a developed chaotic regime. The decay goes faster with increase of ε. To describe the effect quantitatively we introduce a correlation time τ, fitting the true autocorrelation functions by the least squares method to the function $\phi(t)=\phi(0)\exp(-t/\tau)$. Here $\phi(0)$ is taken from the measurements and τ is the only fitting parameter. Validity of the approximation is checked by comparison of the Fourier transform of $\phi(t)$ with the power spectrum of the brightness, connected to each other by the Wiener-Khinchin theorem. The obtained dependence $\tau(\varepsilon)$ is presented in Fig. 2. In agreement with the theory [5,7,11] the experimental dots both below and beyond LP fit at small ε the law $1/\tau \propto \varepsilon$. However, there is an important difference between the dependence $\tau(\varepsilon)$ below and beyond LP. At $f=500$ Hz (below LP) the slope of the straight line $1/\tau(\varepsilon)$ equals 0.61 ± 0.01 s^{-1} and remains the same at any examined values of ε ($0.0254<\varepsilon<0.8059$). At $f=2000$ Hz (beyond LP) the slope is 0.14 ± 0.01 s^{-1} at $\varepsilon<0.08$. Then it increases abruptly to the value 0.68 ± 0.01 s^{-1}, i.e., becomes close to that below LP; cf. Figs. 2(a) and 2(b).

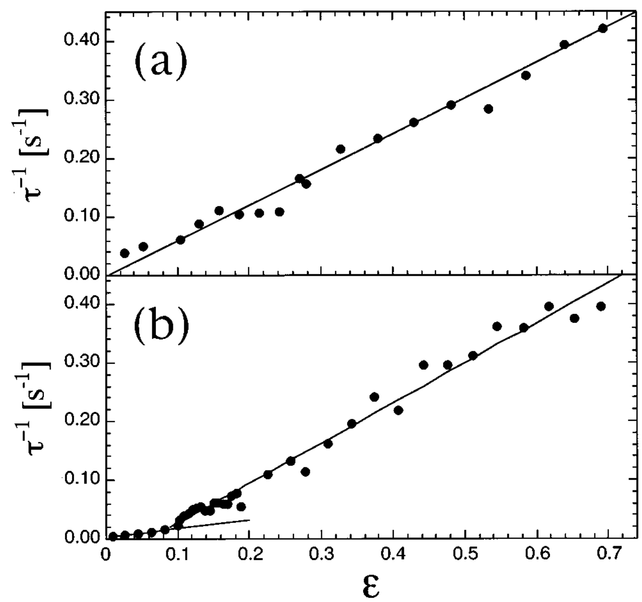

FIG. 2. Inverse correlation time vs ε below the Lifshitz point [(a) $f=500$ Hz] and beyond it [(b) $f=2000$ Hz].

To understand this peculiarity of SMT we conduct observations in a polarized light of steady roll patterns stabilized beyond LP by a magnetic field ($H=2000$ G). The observations show that at $\varepsilon=0.1$ the system undergoes transition from *normal* to *abnormal* rolls. In the abnormal-roll regime $\mathbf{n}_{\parallel}$ is advanced a certain finite angle $\pm\varphi_a$ with respect to the roll's wave vector $\mathbf{k}$, and rolls with the deviation $+\varphi_a$ and $-\varphi_a$ are situated spatially periodically (along the direction parallel to $\mathbf{k}$). It may be supposed that at $H=0$ analogous transition occurs at $\varepsilon=0.08$. The transion affects mutual orientation of local values of $\mathbf{n}_{\parallel}$ and $\mathbf{k}$. If it is the case, transversal orientation of these two vectors results in an additional destabilizing mechanism caused by an uncompensated torque on $\mathbf{n}_{\parallel}$ in the same manner as that below LP. The latter makes the dynamics beyond and below LP similar to each other at $\varepsilon>0.08$.

Stimulating discussions with L. Kramer, A. Rossberg, and W. Pesch are greatly appreciated. M.I.T. is also grateful to M. Mimura and T. Ochiai for being invited to the University of Tokyo and for the provision of excellent conditions to carry out the research. This work is partially supported by the Grant-in-Aid for Scientific Research (Grant No. 08454107) from The Ministry of Education, Science, Sports, and Culture, Japan.

[1] See, e.g., S. Kai and W. Zimmermann, Prog. Theor. Phys. Suppl. **99**, 458 (1989); S. Kai, Forma **7**, 189 (1992); L. Kramer and W. Pesch, Annu. Rev. Fluid Mech. **27**, 515 (1995).
[2] M. C. Cross and P. C. Hohenberg, Rev. Mod. Phys. **60**, 851 (1993).
[3] P. G. de Gennes, and J. Prost, *The Physics of Liquid Crystals* (Clarendon Press, Oxford, 1993); S. Chandrasekhar, *Liquid Crystals* (Cambridge University Press, Cambridge, 1977).
[4] A. Hertrich, W. Decker, W. Pesch, and L. Kramer, J. Phys. (France) II **2**, 1915 (1992).

[5] A. G. Rossberg, A. Hertrich, L. Kramer, and W. Pesch, Phys. Rev. Lett. **76**, 4729 (1996); A. G. Rossberg and L. Kramer, Phys. Scr. **T67**, 121 (1996).

[6] E. D. Siggia and A. Zippelius, Phys. Rev. Lett. **47**, 835 (1981); F. H. Busse and E. W. Bolton, J. Fluid Mech. **146**, 15 (1984); A. J. Bernoff, Euro. J. Appl. Math. **5**, 267 (1994).

[7] M. I. Tribelsky, in *Proceedings of the International Workshop on Nonlinear Dynamics and Chaos, Pohang, Korea, June 1995* [Int. J. Bif. Chaos **7**, 997 (1997)]; M. I. Tribelsky and K. Tsuboi, Phys. Rev. Lett. **76**, 1631 (1996).

[8] M. I. Tribelsky and M. G. Velarde, Phys. Rev. E **54**, 4973 (1996).

[9] H. Sakaguchi, Prog. Theor. Phys. **96**, 1037 (1996).

[10] H. Richter, A. Buka, and I. Rehberg, Phys. Rev. E **51**, 5886 (1995); H. Richter, N. Klöpper, A. Hertrich, and A. Buka, Europhys. Lett. **30**, 37 (1995).

[11] M. I. Tribelsky, K. Hayashi, Y. Hidaka, and S. Kai, *Proceedings of 1st Tohwa Univ. Stat. Phys. Meeting, Fukuoka, Japan, Nov. 1995* [Bussei Kenkyu (Kyoto) **66**, 592 (1996)].

[12] S. Kai, K. Hayashi, and Y. Hidaka, J. Phys. Chem. **100**, 19007 (1996).

[13] G. Küppers and D. Lortz, J. Fluid Mech. **35**, 609 (1969).

[14] M. Dennin, M. Treiber, L. Kramer, G. Ahlers, and D. S. Cannell, Phys. Rev. Lett. **76**, 319 (1996).

[15] Y. Hu, R. E. Ecke, and G. Ahlers, Phys. Rev. Lett. **74**, 5040 (1995).

[16] M. Dennin, D. S. Cannell, and G. Ahlers, Mol. Cryst. Liq. Cryst. Sci. Technol., Sect. A **261**, 337 (1995); M. Dennin, G. Ahlers, and D. S. Cannell, Science **272**, 388 (1996).

[17] For homeotropic EHC it is clear already from the fact that the angular variable φ, which describes the azimuthal orientation of $\mathbf{n}_\parallel$, should be 2π-periodic. In this case even if a certain scale transformation affecting among other variables φ, such as, e.g., $\varphi \to \varphi/\sqrt{\varepsilon}$, could eliminate ε from the governing equations, the periodicity condition for the rescaled φ occurs ε dependent, so ε still enters the problem explicitly [5].

[18] Contrary to our results, spatially chaotic patterns observed by the authors in Refs. [10] beyond LP were identified as steady. The discrepancy may be caused by a variety of reasons, e.g., by the difference in values of material constants of the samples.

[19] In our experiments LP corresponds to $f \approx 1.6$ kHz. Due to similarity between asymptotic-state patterns below and beyond LP, its identification requires a special technique whose details will be reported elsewhere.

[20] The actual sampling rate is 0.1 s. However, comparison of correlation times obtained at different rates shows that change of the rate from 0.1 to 1.0 s, practically, does not affect the value of the correlation time, especially at the most interesting range of small ε. It allows us to employ for the statistical treatment only every 10 successive image of the line.